THE JOURNAL OF PHYSICAL CHEMISTRY C

Article

pubs.acs.org/JPCC

Uniform Mesoporous Anatase–Brookite Biphase TiO_2 Hollow Spheres with High Crystallinity via Ostwald Ripening

Yubao Zhao,[†] Feng Pan,[†] Hui Li,[†] Dongxu Zhao,[§] Lei Liu,[§] Guo Qin Xu,[†,‡] and Wei Chen*[,†,‡,#,¶]

[†]Department of Chemistry, National University of Singapore, 117543, Singapore

[#]Department of Physics, National University of Singapore, 117542, Singapore

[¶]NUS Environmental Research Institute, National University of Singapore, 117411, Singapore

[‡]National University of Singapore (Suzhou) Research Institute, Suzhou, 251123, China

[§]State Key Laboratory of Luminescence and Applications, Changchun Institute of Optics, Fine Mechanics and Physics, Chinese Academy of Sciences, Changchun, 130033, China

Supporting Information

ABSTRACT: With biocompatible oxalic acid as chelating agent, uniform titania hollow spheres were solvothermally obtained. The hollow spheres are composed of 23% brookite phase and 77% anatase phase with good crystallinity. These biphase hollow spheres, possessing large surface area and mesoporousity, form via a typical asymmetric Ostwald ripening mechanism. During this facile process, the oxalic acid plays essential roles in producing the hollow sphere structure, both maintaining the uniformity of the spherical structure and transferring titanium ions during the Ostwald ripening process.

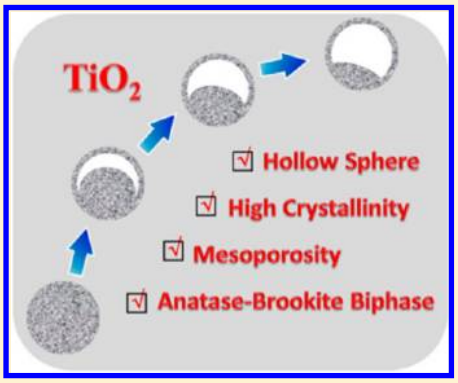

INTRODUCTION

Novel hollow structures have attracted intensive research interest because of their excellent performance and promising application in lithium ion battery, catalysis, and drug delivery.[1−8] TiO_2 has been widely applied in water splitting, organic synthesis, and elimination of water contaminants because of its abundance, nontoxicity, and high efficiency.[9−13] Much effort has been focused on the design and manipulation of the TiO_2 morphologies to study the structure−activity relationship, which can help to reveal the reaction mechanism and hence promote the design of efficient photocatalysts.[14−16] Among various morphologies, TiO_2 hollow structure with controlled shell thickness, mesoporosity, and high crystallinity is attractive for the expected enhanced performance in photocatalysis.

To fabricate the hollow structures, the most popular approach is the sacrificial-template based method, employing polystyrene, silica, carbon, and metal oxides (hard templates), or gas bubble and emulsion micelles etc. (soft templates).[17−22] Despite its wide applicability, the synthesis and removal of the template (by harsh chemical reaction steps or calcination under high temperature) not only complicate the fabrication process but also waste a lot of energy and materials. The other strategy is the recently developed novel self-template routes based on the Kirkendall effect, Galvanic replacement reactions, and Ostwald ripening mechanisms.[1−3] These approaches have stimulated much research interest because the shell formation and core elimination happen simultaneously. For TiO_2 hollow sphere nanostructure, one-pot synthesis based on Ostwald ripening is much more attractive because of the simplicity in synthesis. However, in most of the reported methods, the corrosive halogenide ions, especially fluoride ion, were frequently used for transferring the titanium ions during the Ostwald ripening process. Zeng and co-workers first synthesized hollow anatase sphere through hydrothermal treatment of TiF_4 aqueous solution; by introduction of SnF_4 into TiF_4 aqueous solution, the Sn-doped TiO_2 hollow sphere was obtained.[23,24] $TiCl_4$ and NH_4F were also reported to be feasible for producing TiO_2 hollow spheres.[25,26] A facile and halogenide-free Ostwald ripening approach is highly desirable for both environmental and practical considerations.

Oxalic acid, a biocompatible chemical widely existing in plants and animals, is an effective chelating agent for metal ions, including titanium ion.[27] It is expected that oxalic acid can effectively transfer the titanium ions during Ostwald ripening, and hence the TiO_2 hollow sphere could be obtained in the absence of the corrosive halogenide ions. Herein, we report a facile one-pot solvothermal method for the fabrication of uniform TiO_2 hollow spheres. Oxalic acid was first found to play essential roles in hollowing of titania aggregations. It is

Received: August 20, 2013
Revised: September 25, 2013
Published: October 9, 2013

   dx.doi.org/10.1021/jp408322g | J. Phys. Chem. C 2013, 117, 21718−21723

worth noting that the obtained samples are composed of anatase and brookite phases. These biphase TiO_2 hollow spheres possess mesoporous structure, high crystallinity, and adjustable interior space. It exhibits good catalytic performance in the photocatalytic oxidation reactions.

EXPERIMENTAL SECTION

Synthesis. The TiO_2 hollow sphere was obtained via solvothermal synthesis in *N*,*N*-dimethylformamide (DMF). In a typical synthesis, titanium *n*-butoxide and oxalic acid were dissolved in DMF with concentration of 3.9 mM and 1.1 M, respectively. Seventy-five milliliters of this clear yellow solution was placed in a 100 mL autoclave, and was then subjected to solvothermal conditions at 180 °C for 10 h. The as-synthesized TiO_2 sample was washed with ethanol and dried in vacuum at 80 °C for 4 h, followed by calcination at 500 °C in air for 3 h with the temperature ramping rate of 8 °C/min. The as-synthesized and calcined samples are denoted by THS and THS-500, respectively.

Photocatalytic Reactions. *1. Phenol Degradation.* Ten milligrams of photocatalyst and a 20 mL phenol aqueous solution with a concentration of 25 mg/L were mixed in a Pyrex reactor. After 40 min of stirring in the dark for adsorption−desorption balance, the mixture was illuminated by a 300 W xenon lamp and sampled at certain intervals. The phenol concentration was determined by high-performance liquid chromatography (HPLC) installed with a Dikma C18 column. The mobile phase for HPLC is CH_3CN/H_2O with a ratio of 3/7, and the wavelength for detection is 270 nm.

2. Rhodamine B (RhB) Degradation Reaction. The reaction mixture contained 10 mg of catalyst and 40 mL of Rhodamine B aqueous solution (2×10^{-5} mol/L). The reaction was irradiated by a 300 W xenon lamp, and the RhB concentration was measured by a UV−vis spectrometer.

RESULTS AND DISCUSSION

As shown in the X-ray diffraction (XRD) patterns (Figure 1), the as-synthesized sample (THS) was composed of anatase (JCPDS 21-1272) and brookite (JCPDS 29-1360) phases. The percentage of brookite in the brookite/anatase mixed phase was estimated by the equation[28]

$$r_{\text{Brookite}} = I^{121}_{\text{Brookite}}/(I^{120}_{\text{Brookite}} + I^{101}_{\text{Anatase}}) \times 100\%$$

r_{Brookite} represents the percentage of brookite; $I^{121}_{\text{Brookite}}$ and $I^{120}_{\text{Brookite}}$ represent the area of the brookite (121) and (120) diffraction peaks, respectively; I^{101}_{Anatase} represents the area of the anatase (101) diffraction peak).

Anatase and brookite phases in the as-synthesized sample account for ca. 77% and ca. 23%, respectively. After calcination at 500 °C, THS-500 exhibited enhanced crystallinity compared to the as-synthesized sample, and the average size of anatase and brookite crystals in THS-500 was 14 and 17 nm, respectively (Figure 1f,g). The Brookite ratio in this TSH-500 is ca. 20%. To illuminate the formation process of this biphase structure, the samples solvothermally reacted with different endurance were characterized by XRD. As indicated in Figure 1a, the sample obtained with a reaction time of 3 h was mixed phases of anatase and brookite. Moreover, for the samples with reaction time of 4−10 h, the ratio of anatase to brookite remained constant, although the crystallinity of anatase and brookite enhanced with the reaction time as indicated by the increased diffraction intensity (Figure 1b−f). It is commonly

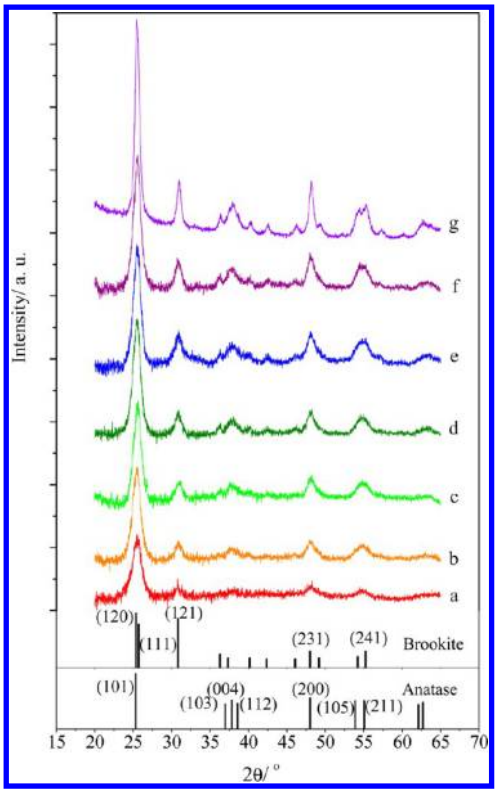

Figure 1. XRD patterns of the TiO_2 hollow spheres obtained at different reaction times: (a) 3 h; (b) 4 h; (c) 5 h; (d) 6 h; (e) 8 h; (f) 10 h; (g) sample (f) calcined at 500 °C for 3 h. At the lower part of the pattern, the single lines state the standard diffraction angles and intensities of anatase and brookite phases.

reported that brookite phase forms with strong acidic conditions, halogenide ions (F^- and Cl^-), a very long aging time period, and high reaction temperature (above 220 °C).[29−35] However, the mild reaction condition in this work also produced both anatase and brookite crystals that formed and grew synchronously, which further expanded our understanding of the formation conditions of the rare brookite phase.

As shown in Figure 2, the TiO_2 spheres are uniform in size and most of them are intact with a diameter of ca. 450 nm (Figure 2a). Occasionally, we could also observe holes existing on the sphere surface, indicating the possibility of hollow sphere structure formation. This prediction could be corroborated by TEM images. The asymmetric hollow sphere structure with a core can be clearly observed and the thickness of the shell is ca. 30 nm (Figure 2b,c). It is worth noting that these hollow spheres are stable against high temperature. After calcination at 500 °C for 3 h, THS-500 with enhanced crystallinity still kept the pristine hollow structure morphology without collapse (Figure 2d). To confirm whether there is any difference in phase composition between different parts of this asymmetrical structure, selected area electron diffraction with electron beam positioned at different regions of the hollow sphere was conducted. All the diffraction patterns reveal that the anatase and brookite phases coexist both in the shell and core parts (Figure 2f−h) of the samples THS and THS-500. Additionally, the HRTEM images of the shell could also clearly demonstrate the coexistence of anatase and brookite crystals in the hollow shell. As shown in Figure 2e and in Figure S1 in the Supporting Information, the spacing of 0.29 and 0.23 nm corresponds to the lattice distance of brookite (121) and

dx.doi.org/10.1021/jp408322g | J. Phys. Chem. C 2013, 117, 21718−21723

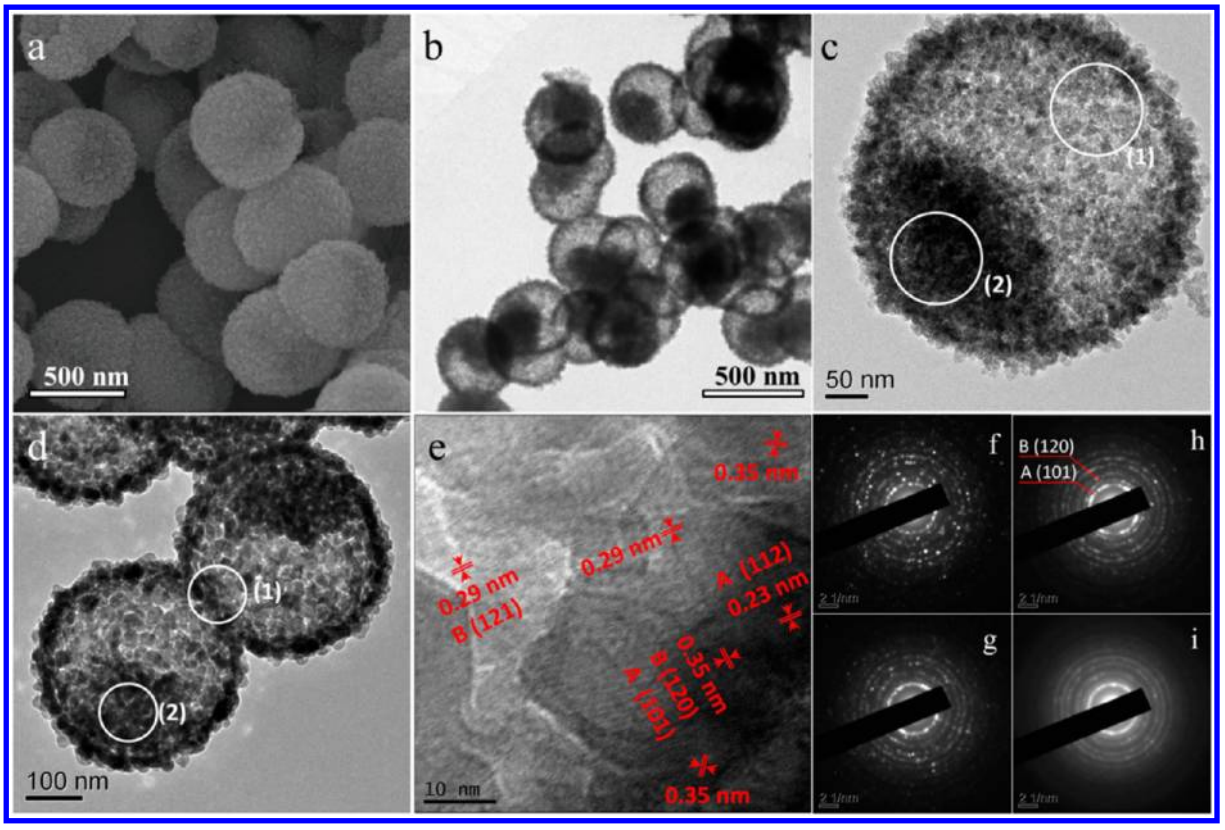

Figure 2. (a–c) SEM and TEM images of the as-synthesized TiO_2 hollow spheres (THS) (d and e) TEM images of the calcined TiO_2 hollow spheres (THS-500); (f–i) selected area electron diffraction (SAED) patterns obtained with the aperture diameter of ca. 100 nm. (f) and (g) are the electron diffraction patterns with the electron beam located at the positions (1) and (2) circled in (d), respectively; (h) and (i) are the electron diffraction patterns with the electron beam positioned at the areas (1) and (2) marked in (c), respectively; "A" and "B" in (h) are the abbreviations for "anatase" and "brookite", respectively. The large-dimension HRTEM images of THS-500 are also available in the Supporting Information (Figure S1).

anatase (112) planes, respectively; and the lattice spacing of 0.35 nm could be attributed to the distance of either anatase (101) planes or brookite (120) planes. Combining with the fact that the ratio of anatase to brookite phases remained constant during the Ostwald ripening process, we suggest that the brookite and anatase phases present uniformly in this asymmetric hollow sphere structure.

The concentrations of titanium *n*-butoxide and oxalic acid were of great importance to the formation of the spherical hollow structure. When the amount of titanium butoxide increased to 19.6 mM, the Ostwald ripening did not occur, and the solid spheres appeared as the final product (Supporting Information, Figure S2). The optimum concentration for titanium butoxide is 3.9 mM. As to oxalic acid, with lower concentration, the initially formed nanoparticles failed to self-assemble into a spherical structure. If the amount of oxalic acid in the reaction solution exceeded 1.4 M, the obtained hollow spheres were not as uniform as that synthesized with the oxalic acid concentrations in the range of 1.1–1.4 M. Apparently, the oxalic acid plays double roles: (1) inducing the nanocrystals to assemble spherically and maintaining the uniformity of the hollow spheres; and (2) acting as chelating agent for titanium ions transfer in core dissolving and shell recrystallizing during the Ostwald ripening process. This process also has high reaction temperature tolerance, and uniform hollow spheres could be obtained under a wide range of 150–180 °C (Supporting Information, Figure S3).

To study the formation mechanism of the titania hollow spheres, we carried out time-dependent reactions and TEM characterizations. As shown in Figure 3a, the initial state of the reaction was spherical aggregation of nanoparticles. In Figure 3b, we can clearly observe that the hollowing asymmetrically started from the side of the sphere beneath the shell, not from the center of the sphere. This indicates that the region beneath the shell is less dense or composed of smaller crystals. The interior space increased with the reaction time until 5 h. However, the hollowing stopped after 5 h of reaction, and the interior space percentage of ca. 60% did not increase as indicated by the TEM images of the samples with the reaction time of 6 and 10 h (Figures 3b–f and 2c), which follows the typical asymmetrical Ostwald ripening mechanism.[36]

Considering the Ostwald ripening process involving core dissolving and shell recrystallizing, the channel for mass transport may finally result in porosity. It is expected that the hollow spheres may possess fine porous structure, which is highly favorable for catalysis. The porosity of the hollow spheres was characterized by N_2 adsorption–desorption. As indicated by the hysteresis loop in the isotherms (Figure 4a), the as-synthesized TiO_2 hollow spheres are mesoporous.[37] Most of the pores have a size smaller than 10 nm, and the maximum size distribution is 3 nm (Figure 4a inset). Because of the presence of these mesopores, the as-synthesized hollow spheres have a quite high BET surface area of 168.3 m^2/g (Table 1). In Figure 4b, the adsorption isotherms of the calcined sample reveals that THS-500 maintained a meso-

dx.doi.org/10.1021/jp408322g | J. Phys. Chem. C 2013, 117, 21718–21723

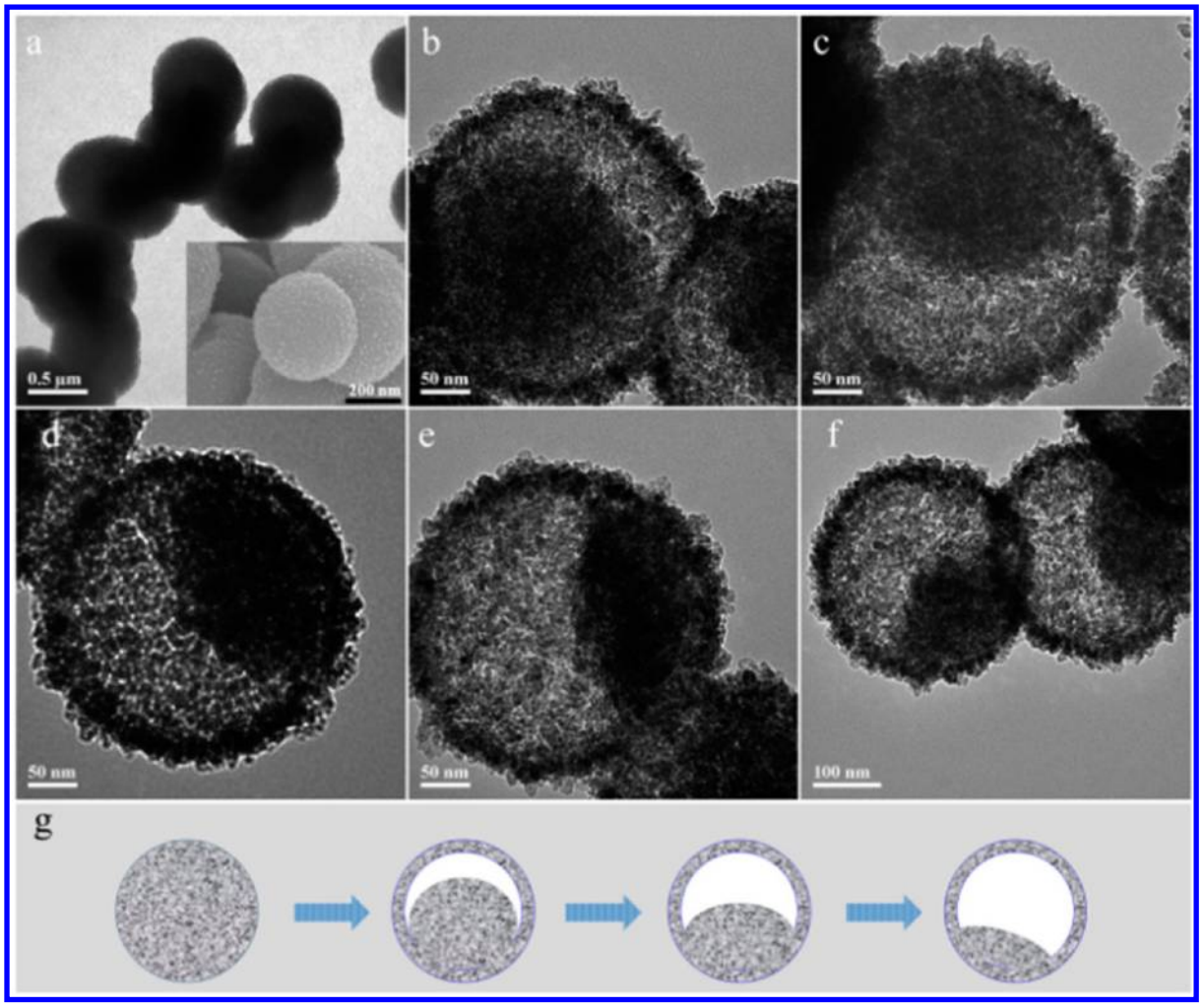

Figure 3. TEM images of the samples with different reaction times: (a) 3 h at 150 °C (to capture the initial state of the fast reaction process, we lower the reaction temperature to get this sample). If not stated, all the reactions are at 180 °C. (b) 2 h; (c) 3 h; (d) 4 h; (e) 5 h; (f) 6 h; (g) Scheme showing the Ostwald ripening process.

porous structure with increased pore size ranging from 4 to 30 nm, and the maximum pore size distribution was 10 nm. The hollow interior space and the mesoporosity make this hollow sphere an ideal material for designing nanoreactors.

To reveal the photocatalytic performance of this novel mesoporous anatase–brookite biphase TiO_2 hollow sphere, the samples were evaluated in the photocatalytic oxidation of phenol and RhB, and commercially available pure anatase nanoparticles were employed as reference photocatalyst. The micrometer-sized as-synthesized TiO_2 hollow sphere exhibited catalytic activity slightly inferior to that of the reference photocatalyst with the reaction rate constant of 0.025 and 0.031 min^{-1}, respectively (Table 1 and Figure S4 in the Supporting Information). After the calcination, although the surface area drastically dropped to 60.1 from 168.3 m^2/g, THS-500 possesses enhanced photocatalytic performance, and the reaction rate constant in phenol degradation increased to 0.030 min^{-1}. In the RhB degradation reaction, despite its relative low surface area, THS-500 exhibited higher photocatalytic performance than the reference photocatalyst with the reaction rate constant of 0.077 and 0.070 min^{-1}, respectively, whereas for the as-synthesized hollow sphere TiO_2, the catalytic performance was comparable to the reference photocatalyst. It is worth noting that the ease of separation of such submicrometer-sized catalyst from the reaction system is of great importance from the perspective of practical applications.

The photocatalytic activity of brookite was reported to be highly sensitive to the morphology, from inactive to highly active.[29,31] The mesoporous anatase–brookite biphase TiO_2 hollow spheres were submicrometer-sized aggregation containing ca. 23% of brookite, while the reference catalyst is monodispersed anatase nanocrystals with average crystal size of ca. 18 nm and large surface area of 107.5 m^2/g (Table 1 and Figure S5 in the Supporting Information). It is expected that the reference catalyst should have catalytic performance superior to that of the submicrometer-sized aggregations. However, the catalytic performance of THS-500 with relatively low surface area was comparable to or sometimes even better than the photocatalytic activity of the reference anatase. Inspired by the mechanism of the improved reactivity of anatase–rutile mixed phases,[38,39] we tentatively believed that anatase–brookite mixed phase may also contribute to the aforementioned enhanced photocatalytic activity.

■ CONCLUSIONS

In this work, we developed a facile one-pot method to fabricate novel mesoporous anatase–brookite biphase TiO_2 hollow spheres via the Ostwald ripening process employing a

dx.doi.org/10.1021/jp408322g | J. Phys. Chem. C 2013, 117, 21718–21723

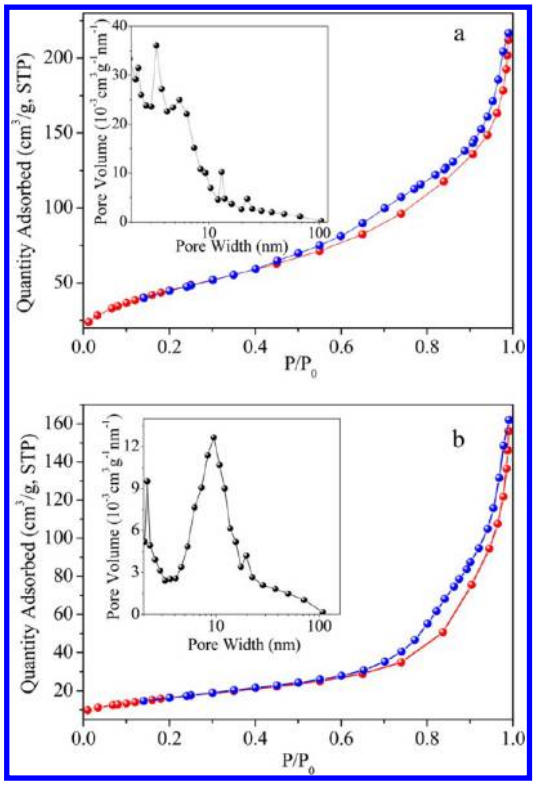

Figure 4. N_2 adsorption−desorption isotherms of the as-synthesized TiO_2 hollow spheres (a) and calcined TiO_2 hollow spheres THS-500 (b). The insets in each figure are their respective pore size distribution patterns.

Table 1. BET Surface Area of the Samples and the Reaction Rate Constant in Phenol and RhB Photo-oxidation Reactions

		reaction rate constant (10^{-3} min^{-1})[b]	
photocatalysts[a]	BET surface area (m^2/g)	phenol	RhB
THS	168.3	25	67
THS-500	60.1	30	77
RC	107.5	31	70

[a]THS, as-synthesized TiO_2 hollow sphere; THS-500, calcined THS; RC, reference catalyst. (Commercially available pure anatase nanoparticles with average crystal size of 18 nm were provided by MTI Corporation.) [b]The reaction rate was calculated based on the presudo-first-order reaction kinetic model at the conversion below 70%. The error of the reaction rate constant for both reactions is $\pm 1 \times 10^{-3}$ min^{-1}.

biocompatible oxalic acid. This biphase structure is composed of ca. 23% brookite and ca. 77% anatase. The submicrometer hollow spheres exhibit good photocatalytic performance in the degradation of phenol and RhB. This method opens a new avenue to simplified fabrication of uniform TiO_2 hollow sphere structure. These unique biphase hollow spheres with mesoporous structure and high crystallinity are ideal for designing nanoreactors.

■ ASSOCIATED CONTENT

Supporting Information

Additional SEM and TEM images. This material is available free of charge via the Internet at http://pubs.acs.org.

■ AUTHOR INFORMATION

Corresponding Author

*E-mail: phycw@nus.edu.sg.

Notes

The authors declare no competing financial interest.

■ ACKNOWLEDGMENTS

We acknowledge the support from Singapore NRF CREATE-SPURc project, MOE grants R143-000-505-112, R143-000-530-112, and R143-000-542-112 and Singapore-Peking-Oxford Research Enterprise, COY-15-EWI-RCFSA/N197-1 rd.

■ REFERENCES

(1) Yin, Y.; Rioux, R. M.; Erdonmez, C. K.; Hughes, S.; Somorjai, G. A.; Alivisatos, A. P. Formation of Hollow Nanocrystals Through the Nanoscale Kirkendall Effect. *Science* **2004**, *304*, 711−714.

(2) Ibez, M.; Cabot, A. All Change for Nanocrystals. *Science* **2013**, *340*, 935−936.

(3) Oh, M. H.; Yu, T.; Yu, S. H.; Lim, B.; Ko, K. T.; Willinger, M. G.; Seo, D. H.; Kim, B. H.; Cho, M. G.; Park, J. H.; Kang, K.; Sung, Y. E.; Pinna, N.; Hyeon, T. Galvanic Replacement Reactions in Metal Oxide Nanocrystals. *Science* **2013**, *340*, 964−968.

(4) Lee, J.; Park, J. C.; Song, H. A Nanoreactor Framework of a Au@SiO_2 Yolk/Shell Structure for Catalytic Reduction of p-Nitrophenol. *Adv. Mater.* **2008**, *20*, 1523−1528.

(5) Zhang, Q.; Zhang, T.; Ge, J.; Yin, Y. Permeable Silica Shell through Surface-Protected Etching. *Nano Lett.* **2008**, *8*, 2867−2871.

(6) Li, J.; Zeng, H. C. Size Tuning, Functionalization and Reactivation of Au in TiO_2 Nanoreactors. *Angew. Chem., Int. Ed.* **2005**, *44*, 4342−4345.

(7) Lou, X. W.; Archer, L. A.; Yang, Z. Hollow Micro-/Nanostructures: Synthesis and Applications. *Adv. Mater.* **2008**, *20*, 3987−4019.

(8) Zhang, Q.; Wang, W.; Goebl, J.; Yin, Y. Self-templated Synthesis of Hollow Nanostructures. *Nano Today* **2009**, *4*, 494−507.

(9) Chen, C.; Ma, W.; Zhao, J. Semiconductor-Mediated Photodegradation of Pollutants under Visible-Light Irradiation. *Chem. Soc. Rev.* **2010**, *39*, 4206−4219.

(10) Fox, M. A.; Dulay, M. T. Heterogeneous Photocatalysis. *Chem. Rev.* **1993**, *93*, 341−357.

(11) Lang, X.; Ji, H.; Chen, C.; Ma, W.; Zhao, J. Selective Formation of Imines by Aerobic Photocatalytic Oxidation of Amines on TiO_2. *Angew. Chem., Int. Ed.* **2011**, *50*, 3934−3937.

(12) Chen, X.; Liu, L.; Yu, P. Y.; Mao, S. S. Increasing Solar Absorption for Photocatalysis with Black Hydrogenated Titanium Dioxide Nanocrystals. *Science* **2011**, *331*, 746−750.

(13) Zhang, M.; Chen, C.; Ma, W.; Zhao, J. Visible-Light-Induced Aerobic Oxidation of Alcohols in a Coupled Photocatalytic System of Dye-Sensitized TiO_2 and TEMPO. *Angew. Chem., Int. Ed.* **2008**, *47*, 9730−9733.

(14) Yang, H. G.; Sun, C. H.; Qiao, S. Z.; Zou, J.; Liu, G.; Smith, S. C.; Cheng, H. M.; Lu, G. Q. Anatase TiO_2 Single Crystals with a Large Percentage of Reactive Facets. *Nature* **2008**, *453*, 638−641.

(15) Zhao, Y.; Ma, W.; Li, Y.; Ji, H.; Chen, C.; Zhu, H.; Zhao, J. The Surface-Structure Sensitivity of Dioxygen Activation in the Anatase-Photocatalyzed Oxidation Reaction. *Angew. Chem., Int. Ed.* **2012**, *51*, 3188−3192.

(16) Wu, N.; Wang, J.; Tafen, D. N.; Wang, H.; Zheng, J. G.; Lewis, J. P.; Liu, X.; Leonard, S. S.; Manivannan, A. Shape-Enhanced Photocatalytic Activity of Single-Crystalline Anatase TiO_2 (101) Nanobelts. *J. Am. Chem. Soc.* **2010**, *132*, 6679−6685.

(17) Joo, J. B.; Zhang, Q.; Lee, I.; Dahl, M.; Zaera, F.; Yin, Y. Mesoporous Anatase Titania Hollow Nanostructures though Silica-Protected Calcination. *Adv. Funct. Mater.* **2012**, *22*, 166−174.

(18) Lou, X. W.; Archer, L. A. A General Route to Nonspherical Anatase TiO_2 Hollow Colloids and Magnetic Multifunctional Particles. *Adv. Mater.* **2008**, *20*, 1853−1858.

(19) Chen, J. S.; Chen, C.; Liu, J.; Xu, R.; Qiao, S. Z.; Lou, X. W. Ellipsoidal Hollow Nanostructures Assembled from Anatase TiO_2 Nanosheets as a Magnetically Separable Photocatalyst. *Chem. Commun.* **2011**, *47*, 2631−2633.
(20) Chen, J. S.; Luan, D.; Li, C. M.; Boey, F. Y. C.; Qiao, S.; Lou, X. W. TiO_2 and SnO_2@TiO_2 Hollow Spheres Assembled from Anatase TiO_2 Nanosheets with Enhanced Lithium Storage Properties. *Chem. Commun.* **2010**, *46*, 8252−8254.
(21) Wang, Z.; Lou, X. W. TiO2 Nanocages: Fast Synthesis, Interior Functionalization and Improved Lithium Storage Properties. *Adv. Mater.* **2012**, *24*, 4124−4129.
(22) Ding, S.; Chen, J. S.; Wang, Z.; Cheah, Y. L.; Madhavi, S.; Hu, X.; Lou, X. W. TiO_2 Hollow Spheres With Large Amount Of Exposed (001) Facets For Fast Reversible Lithium Storage. *J. Mater. Chem.* **2011**, *21*, 1677−1680.
(23) Yang, H. G.; Zeng, H. C. Preparation of Hollow Anatase TiO_2 Nanospheres via Ostwald Ripening. *J. Phys. Chem. B* **2004**, *108*, 3492−3495.
(24) Li, J.; Zeng, H. C. Hollowing Sn-Doped TiO_2 Nanospheres via Ostwald Ripening. *J. Am. Chem. Soc.* **2007**, *129*, 15839−15847.
(25) Shang, S.; Jiao, X.; Chen, D. Template-Free Fabrication of TiO_2 Hollow Spheres and Their Photocatalytic Properties. *ACS Appl. Mater. Interfaces* **2011**, *4*, 860−865.
(26) Pan, H.; Qian, J.; Cui, Y.; Xie, H.; Zhou, X. Hollow Anatase TiO_2 Porous Microspheres with V-Shaped Channels and Exposed (101) Facets: Anisotropic Etching and Photovoltaic Properties. *J. Mater. Chem.* **2012**, *22*, 6002−6009.
(27) Zeng, S.; Tang, K.; Li, T.; Liang, Z.; Wang, D.; Wang, Y.; Zhou, W. Hematite Hollow Spindles and Microspheres: Selective Synthesis, Growth Mechanisms, and Application in Lithium Ion Battery and Water Treatment. *J. Phys. Chem. C* **2007**, *111*, 10217−10225.
(28) Li, J. G.; Ishigaki, T.; Sun, X. Anatase, Brookite, and Rutile Nanocrystals via Redox Reactions under Mild Hydrothermal Conditions: Phase-Selective Synthesis and Physicochemical Properties. *J. Phys. Chem. C* **2007**, *111*, 4969−4976.
(29) Pottier, A.; Chaneac, C.; Tronc, E.; Mazerolles, L.; Jolivet, J. P. Synthesis of Brookite TiO_2 Nanoparticles by Thermolysis of $TiCl_4$ in Strongly Acidic Aqueous Media. *J. Mater. Chem.* **2001**, *11*, 1116−1121.
(30) Zhao, B.; Chen, F.; Huang, Q.; Zhang, J. Brookite TiO_2 Nanoflowers. *Chem. Commun.* **2009**, 5115−5117.
(31) Lin, H.; Li, L.; Zhao, M.; Huang, X.; Chen, X.; Li, G.; Yu, R. Synthesis of High-Quality Brookite TiO_2 Single-Crystalline Nanosheets with Specific Facets Exposed: Tuning Catalysts from Inert to Highly Reactive. *J. Am. Chem. Soc.* **2012**, *134*, 8328−8331.
(32) Arnal, P.; Corriu, R. J. P.; Leclercq, D.; Mutin, P. H.; Vioux, A. Preparation of Anatase, Brookite and Rutile at Low Temperature by Non-hydrolytic Sol-gel Methods. *J. Mater. Chem.* **1996**, *6*, 1925−1932.
(33) Buonsanti, R.; Grillo, V.; Carlino, E.; Giannini, C.; Kipp, T.; Cingolani, R.; Cozzoli, P. D. Nonhydrolytic Synthesis of High-Quality Anisotropically Shaped Brookite TiO_2 Nanocrystals. *J. Am. Chem. Soc.* **2008**, *130*, 11223−11233.
(34) Wang, D.; Liu, L.; Zhang, F.; Tao, K.; Pippel, E.; Domen, K. Spontaneous Phase and Morphology Transformations of Anodized Titania Nanotubes Induced by Water at Room Temperature. *Nano Lett.* **2011**, *11*, 3649−3655.
(35) Ardizzone, S.; Bianchi, C. L.; Cappelletti, G.; Gialanella, S.; Pirola, C.; Ragaini, V. Tailored Anatase/Brookite Nanocrystalline TiO_2. The Optimal Particle Features for Liquid- and Gas-Phase Photocatalytic Reactions. *J. Phys. Chem. C* **2007**, *111*, 13222−13231.
(36) Liu, B.; Zeng, H. C. Symmetric and Asymmetric Ostwald Ripening in the Fabrication of Homogeneous Core−Shell Semiconductors. *Small* **2005**, *1*, 566−571.
(37) Sing, K. S. W.; Everett, D. H.; Haul, R. A. W.; Moscou, L.; Siemieniewska, T. Reporting Physisoption Data for Gas/Solid Systems with Special Reference to the Determination of Surface Area and Porocity. *Pure Appl. Chem.* **1985**, *57*, 603−619.
(38) Li, G.; Dimitrijevic, N. M.; Chen, L.; Nichols, J. M.; Rajh, T.; Gray, K. The Important Role of Tetrahedral Ti^{4+} Sites in the Phase Transformation and Photocatalytic Activity of TiO_2 Nanocomposites. *J. Am. Chem. Soc.* **2008**, *130*, 5402−5403.
(39) Hurum, D. C.; Agrios, A. G.; Gray, K. A.; Rajh, T.; Thurnauer, M. C. Explaining the Enhanced Photocatalytic Activity of Degussa P25 Mixed-Phase TiO_2 Using EPR. *J. Phys. Chem. B* **2003**, *107*, 4545−4549.